



Published in final edited form as:

*Cancer Chemother Pharmacol.* 2014 June ; 73(6): 1137–1146. doi:10.1007/s00280-014-2447-3.

## Mouse pharmacokinetics and metabolism of the curcumin analog, 4-Piperidione,3,5-bis[(2-fluorophenyl)methylene]-acetate(3E,5E) (EF-24; NSC 716993)

Joel M. Reid<sup>a,1</sup>, Sarah A. Buhrow<sup>a</sup>, Judith A. Gilbert<sup>a</sup>, Lee Jia<sup>b</sup>, Mamoru Shoji<sup>c</sup>, James P. Snyder<sup>d</sup>, and Matthew M. Ames<sup>a</sup>

<sup>a</sup>Department of Oncology, Division of Oncology Research, Mayo Clinic, 200 First Street SW, Rochester, MN 55905, USA

<sup>b</sup>Toxicology and Pharmacology Branch, Developmental Therapeutics Program, DCTD, NCI, Rockville, MD 20852, USA

<sup>c</sup>Department of Hematology and Medical Oncology, Winship Cancer Institute, Emory University, Atlanta, GA 30322, USA

<sup>d</sup>Department of Chemistry and Emory Institute for Drug Development, Emory University, 1515 Dickey Drive, Atlanta, GA 30322, USA

### Abstract

**Purpose**—Curcumin, a keto-enol constituent of turmeric, has *in vitro* and *in vivo* antitumor activity. However, *in vivo* potency is low due to poor oral absorption. The mono-carbonyl analog, 3,5-bis[(2-fluorophenyl)methylene]-4-piperidinone acetate (EF-24, NSC 716993), exhibited broad spectrum activity in the NCI anti-cancer cell line screen and potent anti-angiogenesis activity in a HUVEC cell migration assay. The purpose of this study was to characterize the preclinical pharmacology of EF-24 in mice.

**Methods**—EF-24 plasma stability, protein binding, pharmacokinetics and metabolism were characterized utilizing an LC/MS/MS assay.

**Results**—An LC/MS/MS assay that incorporated protein precipitation with methanol, reverse-phase HPLC separation under gradient elution using an aqueous methanol mobile phase containing 0.1% formic acid and positive electrospray ionization detection of the  $m/z$  312 > 149 transition for EF-24. The assay was linear over the range 7.8-1000 nM. Plasma protein binding was > 98% with preferential binding to albumin. EF-24 plasma disposition in mice after i.v. administration of a 10 mg/kg dose was best fit to a 3-compartment open model. The terminal elimination half-life and plasma clearance values were 73.6 min and 0.482 L/min/kg, respectively. EF-24 bioavailability was 60% and 35% after oral and i.p. administration, respectively. NADPH-dependent metabolism of EF-24 loss in liver microsomal preparations yielded several metabolites consistent with EF-24 hydroxylation and reduction.

<sup>1</sup>Author to Whom Correspondence Should Be Addressed: Joel M. Reid, Ph.D., Department of Oncology, Division of Oncology Research, Mayo Clinic, 200 First Street S.W., Rochester, MN 55905; Phone: 507-284-0822; FAX: 507-293-0107; reid.joel@mayo.edu..

**Conflict of Interest:** None

## Keywords

EF-24; curcumin; LC/MS/MS; pharmacokinetics; mouse

---

## INTRODUCTION

Curcumin, a keto-enol tautomer naturally occurring in the spice turmeric, has demonstrated *in vitro* and *in vivo* antitumor activity, but its *in vivo* potency is low due to poor oral absorption [1]. Strategies for improving curcumin bioavailability have included co-administration with agents that inhibit curcumin metabolism, development of novel formulations which increase curcumin solubility and stability, as well as use of structurally modified parent compound [2]. The mono-carbonyl curcumin analog, 3,5-bis[(2-fluorophenyl)methylene]-4-piperidinone acetate (EF-24, NSC 716993) (Figure 1) was the most active compounds identified during synthesis of a series of truncated, symmetrical curcumin analogs designed for improved solubility and increased anti-cancer and anti-angiogenesis activities [1, 3]. EF-24 exhibited broad spectrum activity in the NCI anti-cancer cell line screen with a mean GI<sub>50</sub> of 0.7 μM, a value ten-fold lower than the mean GI<sub>50</sub> of 7.3 for curcumin [1].

Studies to determine the mechanism of action of EF-24 [4-8] indicated that inhibition of tumor cell growth by EF-24 was associated with cell cycle arrest and caspase-mediated apoptosis in human breast cancer [4], prostate cancer [4], colon cancer [7] and gastric adenocarcinoma [7] cell lines. EF-24 had a substantial effect on markers of oxidative stress including depolarization of the mitochondrial membrane, reduction of intracellular GSH and Trx-1, increase in the concentration of ROS [4] and suppression of the NF-κB signaling pathway via direct inhibition of IKK-mediated phosphorylation of IκB [5]. A dose of 200 μg/kg EF-24 inhibited tumor growth *in vivo* by suppression of PI3K and ERK-MAPK pathways and reduced expression of the cancer promoting gene COX-2 [7]. EF-24 also reduced several markers of angiogenesis including VEGF and IL-8 expression, CD31 staining and microvessel density [7]. In addition, the compound disrupts the microtubule cytoskeleton and inhibits HIF-1 [8, 2008], causes radiosensitization of glioma cells [9], potently inhibits the Fanconi anemia pathway (a multi-gene DNA damage response network implicated in cisplatin resistance) along with other analogs [10, 11] and activates the p38 pathway [12]. Conjugates of EF24 have been put to good use. Coupling of the compound to Factor VIIa has demonstrated the ability to target vascular endothelial cells aberrantly expressing tissue factor in rabbit cornea, matrigel and human breast cancer xenografts in athymic nude mice [13, 14]. Glutathione conjugates of both EF24 and EF31 (Figure 1) are as potent as the unconjugated forms at inhibiting proliferation of MDA-MB-435 human breast cancer cells, but they are simultaneously water soluble [15].

Characterization of EF-24 pharmacokinetics and metabolism in preclinical models requires availability of a sensitive, specific assay to determine drug concentrations that are likely to be in the nanomolar range. We herein describe an LC/MS/MS assay for EF-24 that achieves low nanomolar sensitivity required for quantitation of drug concentrations produced in

preclinical pharmacokinetic studies, work presented in preliminary form at the 96<sup>th</sup> Annual Meeting of the American Association for Cancer Research [16].

## MATERIALS AND METHODS

### Chemicals and Reagents

EF-24 and I-MAH-115 were provided by the Department of Chemistry, Emory University, under the award of the RAPID ACCESS TO NCI DISCOVERY RESOURCES (RAND) Program, National Institutes of Health, Bethesda, MD, USA. HPLC-grade methanol and water were purchased from EM Science (Gibbstown, NJ, USA). Formic acid (minimum 95%), dimethyl sulfoxide (DMSO), citrate-phosphate dextrose solution, human serum albumin fatty acid free and gamma-globulin free from fraction V (96-99%), human  $\alpha_1$ -acid glycoprotein purified from Cohn fraction VI (99%),  $\beta$ -nicotinamide adenine dinucleotide phosphate reduced form (NADPH), potassium phosphate dibasic, potassium phosphate monobasic, and magnesium chloride were purchased from Sigma (St. Louis, MO, USA). Dextrose (5%) was purchased from Baxter Healthcare Corporation (Deerfield, IL, USA). Phosphate buffered saline was purchased from Invitrogen (Carlsbad, CA, USA). Heparin sodium 1,000 units/mL was purchased from American Pharmaceutical Partners, Inc. (Los Angeles, CA, USA). Deionized and distilled water was used to prepare buffer solution. DC protein Assay kit catalog number 800-0112 was purchased from BioRad (Hercules, CA, USA). Drug-free human plasma was obtained from healthy volunteers. Rat and mouse whole blood was collected using 10% heparin in citrate-phosphate dextrose solution as an anticoagulant. The plasma was separated by centrifugation (10,000 rpm x3 minutes at 4°C) and stored at -20°C for later analysis. Dog plasma was collected in heparin and was provided by Battelle (Columbus, OH, USA).

### LC/MS/MS Instrumentation

The LC/MS/MS system consisted of a Shimadzu liquid chromatograph (Wood Dale, IL, USA) with two LC-10ADvp pumps (flow rate 0.200 mL/min), and a SIL-10ADvp auto-injector (injection volume 20  $\mu$ L) coupled to a Quattro Micro mass spectrometer fitted with an electrospray ionization (ESI) probe (Waters Corporation, Milford, MA). EF-24 detection was accomplished using multiple reaction monitoring (MRM) in positive ESI mode with parent ion of 312.05 m/z, daughter ion 149.1 m/z, dwell 0.2 sec, cone 35 volts, and collision energy 22 eV. Internal standard (I-MAH-115) detection was made using MRM in positive ESI mode with parent ion of 433.9 m/z, daughter ion of 169.0 m/z, dwell 0.2 sec, cone 27 volts, and collision energy 40 eV. The source temperature, desolvation temperature, cone gas flow, and desolvation gas flow were 100°C, 150°C, 100 L/hr and 250 L/hr, respectively. MS data was collected for 23 minutes after sample injection. Spectra and chromatograms of EF-24 and I-MAH-115 were processed using the MassLynx v3.5 software (Waters Corporation, Milford, MA). Metabolism data were acquired using a full scan function (MS scan) over the range of potential metabolites (50 - 450 m/z). Once the metabolite masses were found a daughter ion scan was run to determine and confirm structure of the metabolite.

### Chromatographic Conditions

Separation of EF-24 and I-MAH-115 was achieved with a NewGuard RP-18 precolumn (15 x 3.2 mm i.d., 7  $\mu$ m) (Chrom Tech, Apple Valley, MN, USA) and a Genesis Lightning C18 analytical column (10 cm x 2.1 mm, 120 $\text{\AA}$ , 4 $\mu$ m) (Jones Chromatography, Lakewood, CO, USA) by gradient elution utilizing the following profile: 0-10 minute 60% A and 40% B, 10-17 minutes 40% A and 60% B, 17-23 minutes 60% A and 40% B, where solvent A was water containing 0.1% formic acid and solvent B was methanol containing 0.1% formic acid. The flow rate was 0.2 ml/min. After sample injection (20  $\mu$ L), the column effluent was diverted to waste for 3 minutes, after which time the flow was switched to the mass spectrometer.

### Sample Preparation

Stock solutions of EF-24 (1.0 mM) and I-MAH-115 (1.0 mM) were prepared in methanol and stored at  $-20^{\circ}\text{C}$ . EF-24 is light sensitive so all solutions were prepared in amber vials or tubes. Working standard solutions were prepared daily by diluting the stock solutions with MeOH and storing on ice. Plasma standards containing EF-24 were prepared by addition of 5.0  $\mu$ l of 0.039 – 5.0  $\mu$ g/ml drug solutions to 200  $\mu$ l of plasma. After vortex mixing, the plasma proteins were precipitated with 400  $\mu$ l methanol and allowed to stand at room temperature for 5 minutes. After centrifugation (10,000 rpm for 3 min) at ambient temperature, the supernatant was transferred to a glass autosampler vial for LC/MS/MS analysis.

### Plasma and Whole Blood Stability

EF-24 was incubated with mouse, rat, dog, and human plasma at  $37^{\circ}\text{C}$  for 24 hours. Aliquots were removed at specified times (5 min, 15 min, 30 min, 1 hr, 2 hr, 4 hr, 6 hr, and 24 hr), transferred to silanized microcentrifuge tubes, immediately frozen and stored at  $-20^{\circ}\text{C}$  until analysis. Incubation solutions of EF-24 with mouse whole blood were prepared in silanized amber glass vials stored on ice for 4 hours. Aliquots were removed at the beginning of the incubation period and at the following times: 5, 15, 30, 60, 120 and 240 minutes. After sedimentation of red blood cells by centrifugation (10,000 rpm for 3 min), plasma was transferred to silanized microcentrifuge tubes, immediately frozen and stored at  $-20^{\circ}\text{C}$  until analysis.

Long-term storage stability was determined in human plasma containing 31 or 1000 nM EF-24 kept in silanized microcentrifuge tubes, frozen, and stored at  $-20^{\circ}\text{C}$  for 28 days. Aliquots (500  $\mu$ l plasma) were periodically removed, thawed and drug content was measured by LC/MS/MS analysis.

### Protein binding

EF-24 binding to proteins was measured in thawed dog, human, mouse, and rat plasma, human serum albumin (40 mg/ml) dissolved in phosphate buffered saline, pH 7.4 and  $\alpha_1$ -acid glycoprotein (1 mg/ml). After 30 minute incubation at  $37^{\circ}\text{C}$ , samples were added to Beckman polycarbonate centrifuge tubes (11x34 mm) and centrifuged in a Beckman TL-100 ultracentrifuge (90,000 rpm x3 hours at  $4^{\circ}\text{C}$ ). EF-24 concentration in the upper portion of the supernatant was analyzed by LC/MS/MS to provide the unbound concentration. To

verify that the supernatant contained no protein, an aliquot was removed and the protein concentration was measured using the DC protein assay (Bio-Rad; Hercules, CA). Drug concentrations were measured in samples before (plasma) and after (supernatant) ultracentrifugation. The percentage of drug recovered and protein binding were calculated by the equations:

$$\text{Percentage Recovered} = \left[ \frac{\text{Filtrate cup concentration}}{\text{Sample reservoir concentration}} \right] \times 100\%$$

$$\text{Protein Binding} = \left[ 1 - \frac{\text{Percentage Recovered(Plasma)}}{\text{Percentage Recovered(Supernatant)}} \right] \times 100\%$$

## Pharmacokinetics

All animal studies were performed under protocols and guidelines approved by the Institutional Animal Care and Use Committee of the Mayo Clinic (Rochester, MN). EF-24 (10 mg/kg) was administered by intravenous (IV), intraperitoneal (IP), and oral (PO) dose to male CD2F<sub>1</sub> mice (19-26 g). For IV dosing, a 10 μM dose of EF-24 was dissolved in D<sub>5</sub>W:DMSO (9:1, v/v) and was injected into the lateral tail vein using a 1-cc syringe fitted with a 27 gauge needle. Blood samples (two mice per time-point) were collected 3, 5, 10, 15, 30, 60, 120 and 240 minutes after administering the dose. For PO and IP dosing, a 3.6 μM dose of EF-24 was dissolved in D<sub>5</sub>W:DMSO (9:1, v/v) and was administered using a 1-cc syringe fitted 20 gauge feeding needle (PO) or a 1-cc syringe fitted 27 gauge needle in the right side of the abdomen, respectively. Blood samples (two mice per time-point) were collected 3, 5, 10, 15, 30, 60, 120, 180, 240, 360 and 480 minutes after administering the dose.

Blood samples were obtained from mice anesthetized under methoxyflurane vapors by cardiac puncture using a 10% heparin in citrate phosphate dextrose solution anticoagulant (150 μl anticoagulant/ml whole blood), transferred to silanized amber microcentrifuge tubes and immediately chilled on ice. After separation by centrifugation (10,000 rpm x 3 min at 4°C) plasma was transferred to silanized amber microcentrifuge tubes and immediately frozen. Samples were assayed for drug content within 2 days of collection.

Half-life values were estimated by compartmental analysis, while area under the plasma concentration-time curve (AUC), clearance and steady-state volume of distribution were estimated by non-compartmental analysis of the mean concentration values, using the program WINNONLIN (version 1.5).

## *In Vitro* Metabolism

Cytochromes P450 were induced in mice by 3-day treatment with dexamethasone (300 mg/kg), phenobarbital (80 mg/kg), or 3-methylcholanthrene (20 mg/kg) intraperitoneally before isolation on day 4. Mouse liver microsomes were isolated by differential centrifugation [17]. Human liver samples, medically unsuitable for transplantation were acquired under the auspices of the Washington Regional Transplant Consortium (Washington, DC), and their preparation and characterization has been previously published [18]. Microsomal suspensions were incubated in amber glass vials maintained at 37°C in a shaker bath. Each incubation mixture (0.1-0.5 ml) contained EF-24 (10 μM), microsomes (0.2 - 1 mg/ml

protein), NADPH (1.0 mM), magnesium chloride (5 mM) and potassium phosphate buffer (100 mM) adjusted to pH 7.4. Identical incubations with active microsomes in which NADPH was omitted served as controls. After pre-incubation of the microsomes with the reaction buffer (+/- NADPH) for two minutes, the metabolic process was initiated by adding EF-24. To assess oxygen dependence, the procedure was followed as described except that oxygen was depleted by purging the vials with nitrogen before the addition of EF-24. Reactions were terminated after 15-60 minutes incubation by mixing with ice-cold methanol (2:1, v/v) and kept frozen until analysis.

## RESULTS

### Chromatographic conditions

EF-24 was measured in *in vitro* and *in vivo* samples using an LC/MS/MS assay developed in our laboratory. Protonated molecular ion ( $[M+H]^+$ ) intensities for EF-24 and the internal standard were greatest under positive electrospray ionization with a 35 V cone voltage and 22 eV collision energy. Mass spectra for EF-24 (Figure 2a) and the internal standard (Figure 2b) included prominent parent ion  $[M+H]^+$  peaks at  $m/z$  312 and 433, respectively. Prominent product ions for EF-24 and the internal standard were found at  $m/z$  149 and 169, respectively. Based on these data, quantification of EF-24 was performed in the Multiple Reaction Monitoring (MRM) mode by monitoring the  $m/z$  312 $\rightarrow$ 149 transition for EF-24 and the  $m/z$  433 $\rightarrow$ 169 transition for the internal standard. Satisfactory chromatography was achieved and ionization suppression substantially reduced by gradient elution from 40:60 methanol:water with 0.1% formic acid to 60:40 methanol:water with 0.1% formic acid. The retention times of EF-24 and I-MAH-115 under these conditions were 9.3 min and 13.6 min, respectively (Figure 2c and 2d). Standard curves were linear in the range 7.8-2000 nM with  $r^2$  values of  $> 0.9900$  and a lower limit of quantitation of 7.8 nM.

### Stability

A second peak with a fragmentation pattern similar to that of the parent molecule was observed in chromatograms of EF-24 during initial assay development. Formation of that peak was attributed to light sensitivity of EF-24, since it was prevented by wrapping tubes in aluminum foil or by using amber glass vials and amber plastic tubes.

Stability of EF-24 in human, mouse, rat, and dog plasma was evaluated at 4°C and 37°C for a 24-hour period (Table 1). EF-24 was stable in human and rat plasma, but modest loss of EF-24 was observed in mouse and dog plasma where half-life values were 11 and 35 hours, respectively (Table 1). EF-24 long term stability in plasma stored frozen at -20°C was  $> 32$  days.

In preparation for pharmacokinetic experiments, EF-24 partition ratio and stability were determined in fresh mouse whole blood. When identical amounts of EF-24 were added to equal volumes of plasma and whole blood over the range of 3.9 – 2000 nM, the concentration of EF-24 in plasma isolated from the whole blood sample was equal to that found when EF-24 was added directly to plasma. This observation is consistent with diffusion of EF-24 into red blood cells and indicates a 1:1 partition ratio between plasma and



red blood cells. Multi-exponential loss of EF-24 was observed during 24-hour incubation of EF-24 in whole blood at 37°C. The initial rapid loss of drug during incubation at 37°C was reduced substantially when blood samples were incubated on ice. These data indicate that blood samples should be chilled and processed immediately after collection for pharmacokinetic studies to prevent ex vivo degradation.

### Protein Binding

EF-24 plasma protein binding was evaluated in human, dog, rat, and mouse plasma, as well as in aqueous solutions containing human serum albumin and  $\alpha_1$ -acid glycoprotein (Table 1). Protein binding in human, dog, rat and mouse plasma was 94% or greater for all concentrations. The percent bound value was 95-100% in human serum albumin and < 20% to  $\alpha_1$ -acid glycoprotein, and thus suggests that EF-24 is mostly bound to albumin in plasma.

### Pharmacokinetics

EF-24 pharmacokinetics were characterized in male CD2F<sub>1</sub> mice after intravenous, oral and intraperitoneal administration of a 10 mg/kg dose. EF-24 plasma disposition after i.v. administration was best fit to a 3-compartment open model (Figure 3a). The terminal elimination half-life and plasma clearance values were 73.6 min and 0.482 L/min/kg, respectively (Table 2). EF-24 absorption was rapid after both oral and i.p. administration. Peak plasma concentrations approaching 1000 nM were detected 3 min after the dose was given (Figure 3b and 3c, respectively). Half-life values of ~200 min after oral and i.p. administration were slower than the value observed after i.v. administration. Of note, a secondary peak concentration was observed 360 minutes after administering the i.p. dose. EF-24 bioavailability, determined by comparison of AUC values was 60% and 35% after oral and i.p. administration, respectively. EF-24 was not detected in the 24-hour pooled urine from mice administered 25 mg/kg (n = 2) or 32 mg/kg (n = 2) EF-24 intravenously.

### In Vitro Metabolism

Following 15-minute incubation with mouse liver microsomal preparations, 40%, 41%, and 54% of EF-24 added to the preparations was consumed by NADPH-dependent metabolism in liver microsomal preparations from untreated, PB-pretreated, and 3MC-pretreated mice, respectively (Figure 4a). In human liver microsomes, >70% of added EF-24 was consumed by NADPH-dependent metabolism (Figure 4a).

Several EF-24 metabolites were detected in the mouse and human liver microsomal incubations. Two aromatic ring hydroxylation products were detected in mouse (Figure 4b) and human (Figure 4c) preparations based on presence of a molecular ion with m/z 328 and a daughter ion with m/z 125. Both molecular and product ions were 16 mass units higher than those of EF-24 (m/z 312) indicative of hydroxylation. Formation of both hydroxylated metabolites in mouse liver microsomal preparations was greater in liver microsomes from 3MC-treated mice than from microsomes isolated from phenobarbital-treated mice or untreated mice consistent with metabolism of EF-24 by CYP1A isoforms.

A small amount of a reduced contaminant (m/z 314) was detected in the EF-24 stock, consistent with addition of hydrogen across one of the double bonds (data not shown). This

product co-elutes with EF-24 ( $t_r = 7.4$  min) and was detected when EF-24 was dissolved in buffer with or without added NADPH or microsomes. A second reduced metabolite ( $m/z$  314) that elutes after EF-24 ( $t_r = 10.7$  min) was detected in human (Figure 4d), but not mouse, liver microsomal preparations only in the presence of NADPH, and its formation was time-dependent.

Three peaks with  $m/z$  316 were detected in MS chromatograms from human liver microsomal preparations (Figure 4e). Presence of an ion with  $m/z$  151 in the daughter ion scan for these metabolites was consistent with reduction of EF-24 (Figure 4e). Formation of all three  $m/z$  316 metabolites was dependent on NADPH, but not oxygen. Multiple metabolites with  $m/z$  316 may be due to introduction of 2 chiral centers following reduction.

An unknown metabolite with  $m/z$  298 (Figure 4f) has been detected only in human liver microsomes. This major metabolite is dependent on NADPH in the absence of oxygen. While we have not been able to interpret the MS scan sufficiently to fully identify the structure (Figure 4f), one reasonable alternative is depicted as EF24-5 (Figure 1). It can be rationalized by N-hydroxylation and N-dealkylation of mono-unsaturated EF24-H2 (Figures 1 and 4f) [19] followed by ring closure and elimination of hydroxylamine.

## DISCUSSION

The curcumin analog, EF-24, exhibited broad spectrum antiproliferative activity in cancer cell lines and potent growth inhibition of the HCT-116 human colon tumor xenograft in mice with little apparent toxicity. As with curcumin, growth inhibition has been attributed to a number of biological effects including induction of oxidative stress, suppression of the NF- $\kappa$ B, PI3K and ERK-MAPK pathways, reduced expression of the cancer promoting gene COX-2 and inhibition of angiogenesis. Thus, EF-24 is a candidate for further development. The purpose of this study was to characterize the pharmacokinetics and metabolism of EF-24 in mice to determine whether effective concentrations can be achieved; to determine the most effective route of administration to achieve desired therapeutic concentrations of active compound in clinical trials; and to investigate EF-24 metabolism using rodent and human *in vitro* models in an attempt to predict the effect of metabolism on plasma clearance in clinical trials.

Accordingly, a sensitive, specific LC/MS/MS method was developed for measurement of EF-24 in biological fluids. Ionization conditions were selected to take advantage of prominent product ions for EF-24 and the internal standard under positive electrospray ionization. During assay development, we found that EF-24 was light-sensitive and ionization was sensitive to constituents in plasma. To minimize degradation due to light assay methodology included wrapping samples in aluminum foil after collection in the pharmacokinetic studies, sample preparation in amber vials and minimum exposure to light at other times. Gradient elution was utilized to overcome ionization suppression by plasma constituents that eluted early in chromatograms under isocratic conditions and suppressed signal intensity. As a result of these precautions, a lower limit of quantification of 7.8 nM was achieved with the assay. Furthermore, EF-24 had limited stability in blood that required sample processing immediately after specimen collection. These adaptations permitted



sufficient sensitivity to characterize the EF-24 pharmacokinetics in mice administered a 10 mg/kg dose.

EF-24 pharmacokinetics were characterized in male CD2F<sub>1</sub> mice following i.v., i.p. and oral administration of a 10 mg/kg dose. The peak plasma concentration of 2.5  $\mu$ M EF-24 in mice administered an i.v. dose was well above the *in vitro* GI<sub>50</sub> value for sensitive cell lines in the NCI 60 cell line screen, as well as the concentrations used for *in vitro* studies performed to define EF-24 mechanism of action. Intraperitoneal and oral administration yielded peak plasma concentrations in the range of the *in vitro* GI<sub>50</sub> value, as well as the concentrations used for *in vitro* studies performed to define EF-24 mechanism of action. The reasons for the rapid absorption are unclear, however, it is unlikely that DMSO contributed to enhanced absorption since it had no effect on absorption of other hydrophobic drugs in an intestinal permeability model. [20] The prolonged exposure and high bioavailability of EF-24 after the oral route indicate this would be an effective route of administration to achieve desired therapeutic concentrations of active compound in animal models and clinical trials. Prolonged plasma elimination in mice after oral administration suggests drug may be administered by intermittent dosing using this route.

The high oral bioavailability of EF-24 contrasts markedly with the extremely low oral bioavailability of curcumin in rodents [21, 22] and humans [23-25] where only trace concentrations of curcumin are detected following oral administration. The low bioavailability of curcumin is mainly due to poor absorption since metabolite concentrations, primarily glucuronide and sulfate conjugates [21-25] are also low. The high clearance that exceeded liver blood flow rate and the large volume of distribution suggest that EF-24 undergoes rapid metabolism and extensive tissue distribution following the i.v. dose.

Our studies of EF-24 metabolism focused on oxidative and reductive metabolism by mouse and human liver microsomal preparations. NADPH-dependent loss of EF-24 is consistent with a role for cytochrome P450 in metabolism of EF-24. A proposed scheme of metabolism is illustrated in Figure 4g. At equivalent protein concentrations, metabolism of EF-24 was much greater in human than in mouse liver microsomes. Absence of a difference in metabolism with microsomes from untreated and phenobarbital-treated mice suggest that inducible mouse P450s and their human orthologs such as CYP3A and CYP2B do not contribute substantially to EF-24 metabolism. In contrast, greater metabolism in microsomes from 3MC-treated mice suggests that CYP1A isoforms catalyze EF-24 hydroxylation in mice and homologous CYP1A isoforms catalyze EF-24 hydroxylation in humans.

Reduced metabolites were detected in the human, but not mouse, microsomal incubations. These data suggest that reduction is the predominant route of EF-24 metabolism in humans. The mechanism underlying the species-dependence of EF-24 reduction remains to be elucidated. Reduced metabolites and conjugation products were also detected during pharmacokinetic and *in vitro* metabolism studies with curcumin [21-27]. As with curcumin, EF-24 reduction continued until all of the double bonds were saturated [21, 22, 24, 25].

In conclusion, plasma concentrations of EF-24 associated with *in vitro* pharmacological activity and antitumor effect were achieved with doses that are both tolerable and active in these species. EF-24 has high oral bioavailability in mice. Oxidation, in part catalyzed by CYP1A isoforms, and reduction contribute to EF-24 *in vitro* metabolism.

Independent studies on closely related analogs of EF24, EF31 and UBS-109 (Figure 1), performed toward the conclusion of the present work both supplement and confirm the present observations. For example, EF31 has been compared to EF24 and curcumin in an inflammatory model using mouse RAW264.7 macrophages to show that the former is a 7 – and >10-fold more potent blocker of the NF- $\kappa$ B pathway activity than the other two substances, respectively. Downstream pro-inflammatory mediators, including tumor necrosis factor- $\alpha$ , interleukin-1 $\beta$ , and interleukin-6, were also more effectively obstructed by EF31 vs. EF24, as was the inhibition of IKK $\beta$  (by ~65 fold) [28]. Another study examined the effects of the two analogs on human head and neck squamous cell carcinoma (SCC) Tu212 xenograft tumors established in athymic nude mice. The more soluble EF31 provided a dose-response at 15 and 25 mg/kg i.p. and average AUC(0- $\infty$ ) values of 3386 and 7769 h x ng mL<sup>-1</sup>, respectively [29]. UBS-109 likewise showed a dose response at 50, 100 and 150 mg/kg p.o. on SCC Tu212 xenografts, and 10 and 20 mg/kg i.p. on human pancreatic carcinoma MiPaPc xenografts in athymic nude mice [Manuscripts in preparation 2013]. In a final and very recent investigation of bone mass loss, curcumin, EF31 and UBS109 were compared for their relative effects on osteoblastogenesis and osteoclastogenesis *in vitro*. EF31 and UBS109 revealed a suppressive effect on osteoclastogenesis as compared with curcumin, while UBS109 had a unique stimulatory effect on osteoblastic differentiation and mineralization associated with Smad signaling. The same compound potentially inhibits NF- $\kappa$ B which plays a pivotal role in osteoclastogenesis [30].

These investigations complement the present work and reinforce the conclusion that this class of compounds represents an intriguing area for future development.

## Acknowledgement

MS and JPS are grateful to Dennis Liotta (Emory University) for generous support of preparation of the curcumin analogs.

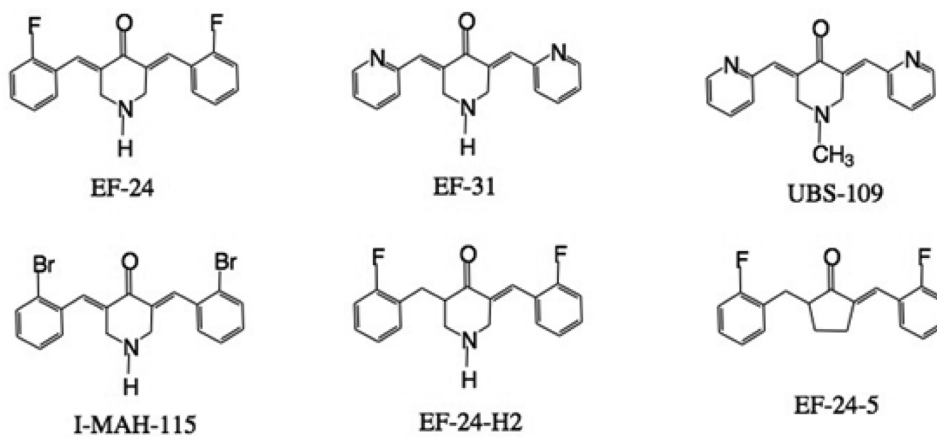
Supported by National Cancer Institute Contract N01-CM-07105, US Department of Defense, Division of US Army DAMD17-00-1-0241 (MS and JPS), BC074220 (MS and JPS) and National Cancer Institute 5 R21 (CA139035-2 (MS and JPS)

## REFERENCES

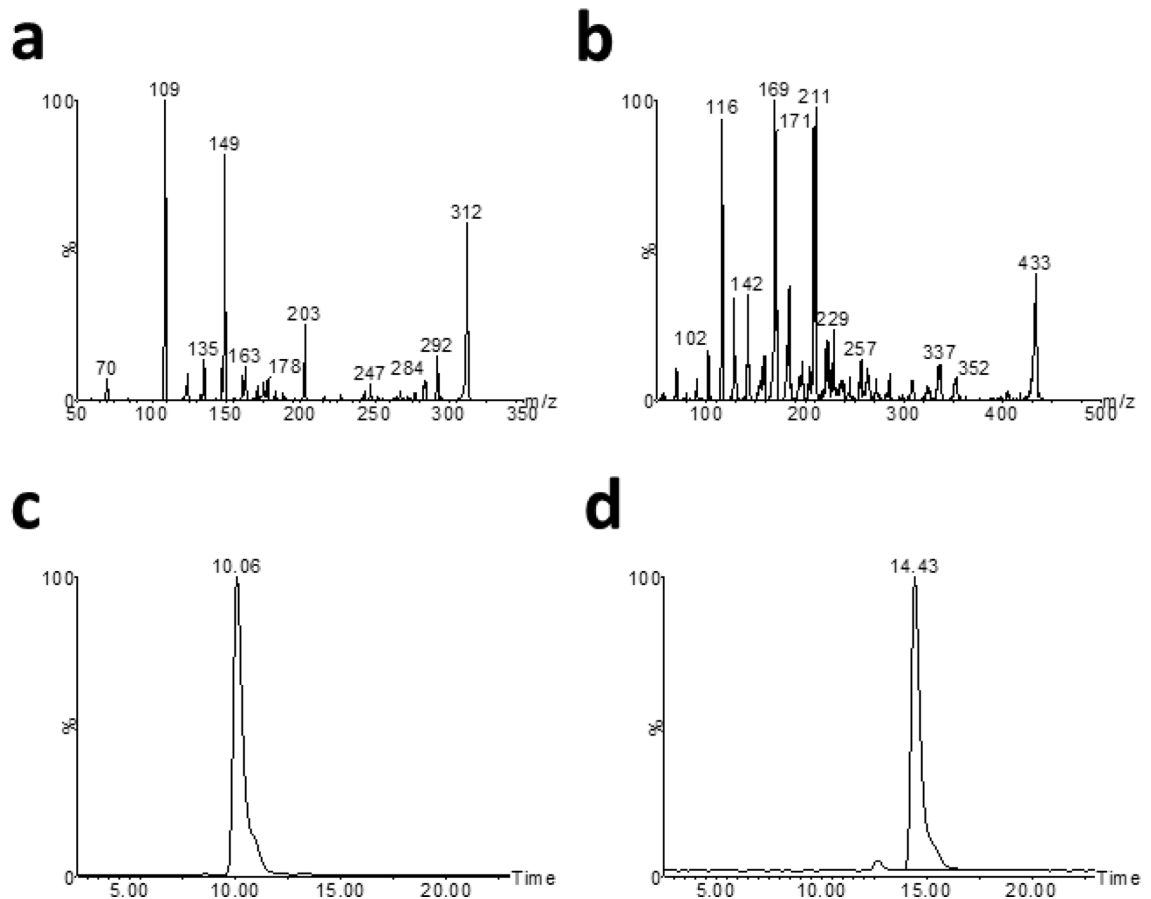
1. Adams BK, Ferstl EM, Davis MC, Herold M, Kurtkaya S, Camalier RF, Hollingshead MG, Kaur G, Sausville EA, Rickles FR, Snyder JP, Liotta DC, Shoji M. Synthesis and biological evaluation of novel curcumin analogs as anti-cancer and anti-angiogenesis agents. *Bioorg Med Chem.* 2004; 12:3871–83. [PubMed: 15210154]
2. Anand P, Kunnumakkara AB, Newman RA, Aggarwal BB. Bioavailability of curcumin: problems and promises. *Mol Pharm.* 2007; 4:807–18. [PubMed: 17999464]
3. Mosley CA, Liotta DC, Snyder JP. Highly active anticancer curcumin analogues. *Adv Exp Med Biol.* 2007; 595:77–103. [PubMed: 17569206]

4. Adams BK, Cai J, Armstrong J, Herold M, Lu YJ, Sun A, Snyder JP, Liotta DC, Jones DP, Shoji M. EF24, a novel synthetic curcumin analog, induces apoptosis in cancer cells via a redox-dependent mechanism. *Anticancer Drugs*. 2005; 16:263–75. [PubMed: 15711178]
5. Kasinski AL, Du Y, Thomas SL, Zhao J, Sun SY, Khuri FR, Wang CY, Shoji M, Sun A, Snyder JP, Liotta D, Fu H. Inhibition of IkappaB kinase-nuclear factor-kappaB signaling pathway by 3,5-bis(2-fluorobenzylidene)piperidin-4-one (EF24), a novel monoketone analog of curcumin. *Mol Pharmacol*. 2008; 74:654–61. [PubMed: 18577686]
6. Selvendiran K, Tong L, Vishwanath S, Bratasz A, Trigg NJ, Kutala VK, Hideg K, Kuppusamy P. EF24 induces G2/M arrest and apoptosis in cisplatin-resistant human ovarian cancer cells by increasing PTEN expression. *J Biol Chem*. 2007; 282:28609–18. [PubMed: 17684018]
7. Subramaniam D, May R, Sureban SM, Lee KB, George R, Kuppusamy P, Ramanujam RP, Hideg K, Dieckgraefe BK, Houchen CW, Anant S. Diphenyl difluoroketone: a curcumin derivative with potent in vivo anticancer activity. *Cancer Res*. 2008; 68:1962–9. [PubMed: 18339878]
8. Thomas SL, Zhong D, Zhou W, Malik S, Liotta D, Snyder JP, Hamel E, Giannakakou P. EF24, a novel curcumin analog, disrupts the microtubule cytoskeleton and inhibits HIF-1. *Cell Cycle*. 2008; 7:2409–17. [PubMed: 18682687]
9. Shu HG, Brown A, Yoon Y, Gao H, Purcell J, Snyder JP, Liotta DC, Shim H. Radiosensitization of glioma cells with the curcumin analogs EF24 and UBS109. Abstract, AACR 99th Annual Meeting. 2008
10. Landais I, Hiddingh S, McCarroll M, Yang C, Sun A, Turker MS, Snyder JP, Hoatlin ME. Monoketone analogs of curcumin, a new class of Fanconi anemia pathway inhibitors. *Mol Cancer*. 2009; 8:133. [PubMed: 20043851]
11. Kachnic LA, Li L, Fournier L, Willers H. Fanconi anemia pathway heterogeneity revealed by cisplatin and oxaliplatin treatments. *Cancer Lett*. 2010; 292:73–9. [PubMed: 20034732]
12. Thomas SL, Zhao J, Li Z, Lou B, Du Y, Purcell J, Snyder JP, Khuri FR, Liotta D, Fu H. Activation of the p38 pathway by a novel monoketone curcumin analog, EF24, suggests a potential combination strategy. *Biochem Pharmacol*. 2010; 80:1309–16. [PubMed: 20615389]
13. Shoji M, Sun A, Kisiel W, Lu YJ, Shim H, McCarey BE, Nichols C, Parker ET, Pohl J, Mosley CA, Alizadeh AR, Liotta DC, Snyder JP. Targeting tissue factor-expressing tumor angiogenesis and tumors with EF24 conjugated to factor VIIa. *J Drug Target*. 2008; 16:185–97. [PubMed: 18365880]
14. Sun A, Shoji M, Lu YJ, Liotta DC, Snyder JP. Synthesis of EF24-tripeptide chloromethyl ketone: a novel curcumin-related anticancer drug delivery system. *J Med Chem*. 2006; 49:3153–8. [PubMed: 16722634]
15. Sun A, Lu YJ, Hu H, Shoji M, Liotta DC, Snyder JP. Curcumin analog cytotoxicity against breast cancer cells: exploitation of a redox-dependent mechanism. *Bioorg Med Chem Lett*. 2009; 19:6627–31. [PubMed: 19854644]
16. Buhrow SA, Reid JM, Jia L, Shoji M, Snyder JP, Liotta DC, Ames MM. LC/MS/MS assay and mouse pharmacokinetics and metabolism of the novel curcumin analog EF-24 (NSC 716993). *Proc Am Assoc Cancer Res*. 2005; 46 Abstract #4169.
17. Ernster L, Siekevitz P, Palade GE. Enzyme-structure relationships in the endoplasmic reticulum of rat liver. *J Cell Biol*. 1962; 15:541–562. [PubMed: 19866614]
18. Harris JW, Rahman A, Kim BR, Guengerich FP, Collins JM. Metabolism of taxol by human hepatic microsomes and liver slices: participation of cytochrome P450 3A4 and an unknown P450 enzyme. *Cancer Res*. 1994; 54:4026–4035. [PubMed: 7913410]
19. Hanson KL, VandenBrink BM, Babu KN, Allen KE, Nelson WL, Kunze KL. Sequential metabolism of secondary alkyl amines to metabolic-intermediate complexes: opposing roles for the secondary hydroxylamine and primary amine metabolites of desipramine, (s)-fluoxetine, and N-desmethyldiltiazem. *Drug Metab Dispos*. 2010; 38:963–72. [PubMed: 20200233]
20. Venkatesh G, Ramanathan S, Nair NK, Mansor SM, Sattar MA, Khan MA, Navaratnam V. Permeability of atenolol and propranolol in the presence of dimethyl sulfoxide in rat single-pass intestinal perfusion assay with liquid chromatography/UV detection. *Biomed Chromatogr*. 2007; 21:484–90. [PubMed: 17294505]

21. Ireson C, Orr S, Jones DJ, Verschoyle R, Lim CK, Luo JL, Howells L, Plummer S, Jukes R, Williams M, Steward WP, Gescher A. Characterization of metabolites of the chemopreventive agent curcumin in human and rat hepatocytes and in the rat in vivo, and evaluation of their ability to inhibit phorbol ester-induced prostaglandin E2 production. *Cancer Res.* 2001; 61:1058–64. [PubMed: 11221833]
22. Pan MH, Huang TM, Lin JK. Biotransformation of curcumin through reduction and glucuronidation in mice. *Drug Metab Dispos.* 1999; 27:486–94. [PubMed: 10101144]
23. Sharma RA, McLelland HR, Hill KA, Ireson CR, Euden SA, Manson MM, Pirmohamed M, Marnett LJ, Gescher AJ, Steward WP. Pharmacodynamic and pharmacokinetic study of oral Curcuma extract in patients with colorectal cancer. *Clin Cancer Res.* 2001; 7:1894–900. [PubMed: 11448902]
24. Sharma RA, Euden SA, Platton SL, Cooke DN, Shafayat A, Hewitt HR, Marczylo TH, Morgan B, Hemingway D, Plummer SM, Pirmohamed M, Gescher AJ, Steward WP. Phase I clinical trial of oral curcumin: biomarkers of systemic activity and compliance. *Clin Cancer Res.* 2004; 10:6847–54. [PubMed: 15501961]
25. Vareed SK, Kakarala M, Ruffin MT, Crowell JA, Normolle DP, Djuric Z, Brenner DE. Pharmacokinetics of curcumin conjugate metabolites in healthy human subjects. *Cancer Epidemiol Biomarkers Prev.* 2008; 17:1411–7. [PubMed: 18559556]
26. Ireson CR, Jones DJ, Orr S, Coughtrie MW, Boocock DJ, Williams ML, Farmer PB, Steward WP, Gescher AJ. Metabolism of the cancer chemopreventive agent curcumin in human and rat intestine. *Cancer Epidemiol Biomarkers Prev.* 2002; 11:105–11. [PubMed: 11815407]
27. Garcea G, Jones DJ, Singh R, Dennison AR, Farmer PB, Sharma RA, Steward WP, Gescher AJ, Berry DP. Detection of curcumin and its metabolites in hepatic tissue and portal blood of patients following oral administration. *Br J Cancer.* 2004; 90:1011–5. [PubMed: 14997198]
28. Olivera A, Moore TW, Sun A, Liotta DC, Snyder JP, Shim H, Marcus AL, Miller AH, Pace TW. Inhibition of the NF- $\kappa$ B signaling pathway by the curcumin analog, 3,5-Bis(2-pyridinylmethylidene)-4piperidone (EF31): anti-inflammatory and anti-cancer properties. *Int Immunopharmacol.* 2010; 12:368–377. [PubMed: 22197802]
29. Zhu S, Moore TW, Lin X, Morii N, Mancini A, Howard RB, Culver D, Arrendale RF, Reddy P, Evers TJ, Zhang H, Sica G, Chen ZG, Sun A, Fu H, Khuri FR, Shin DM, Snyder JP, Shoji M. Synthetic curcumin analog EF31 inhibits the growth of head and neck squamous cell carcinoma xenografts. *Integr Biol (Camb).* 2012; 4:633–40. [PubMed: 22532032]
30. Yamaguchi M, Moore TW, Sun A, Snyder JP, Shoji M. Novel curcumin analogue UBS109 potently stimulates osteoblastogenesis and suppresses osteoclastogenesis: involvement in Smad activation and NF- $\kappa$ B inhibition. *Integr Biol (Camb).* 2012; 4:905–13. [PubMed: 22751853]

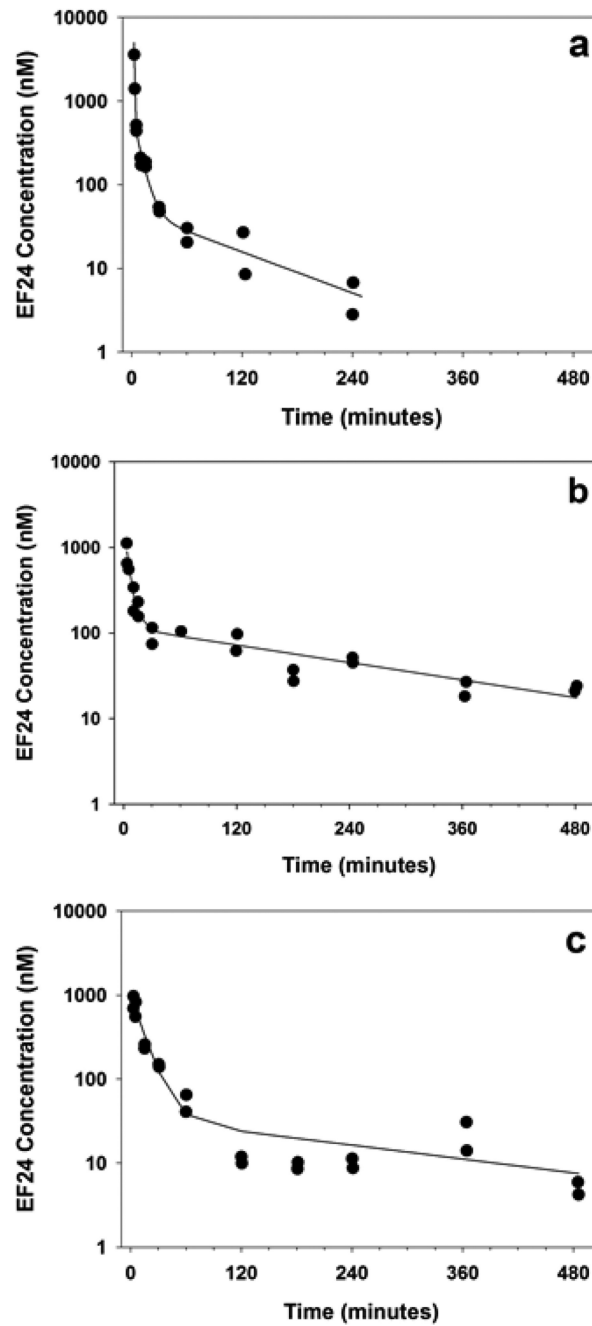


**Fig 1.**  
Structures of EF-24, analogs and internal standard (I-MAH-115)

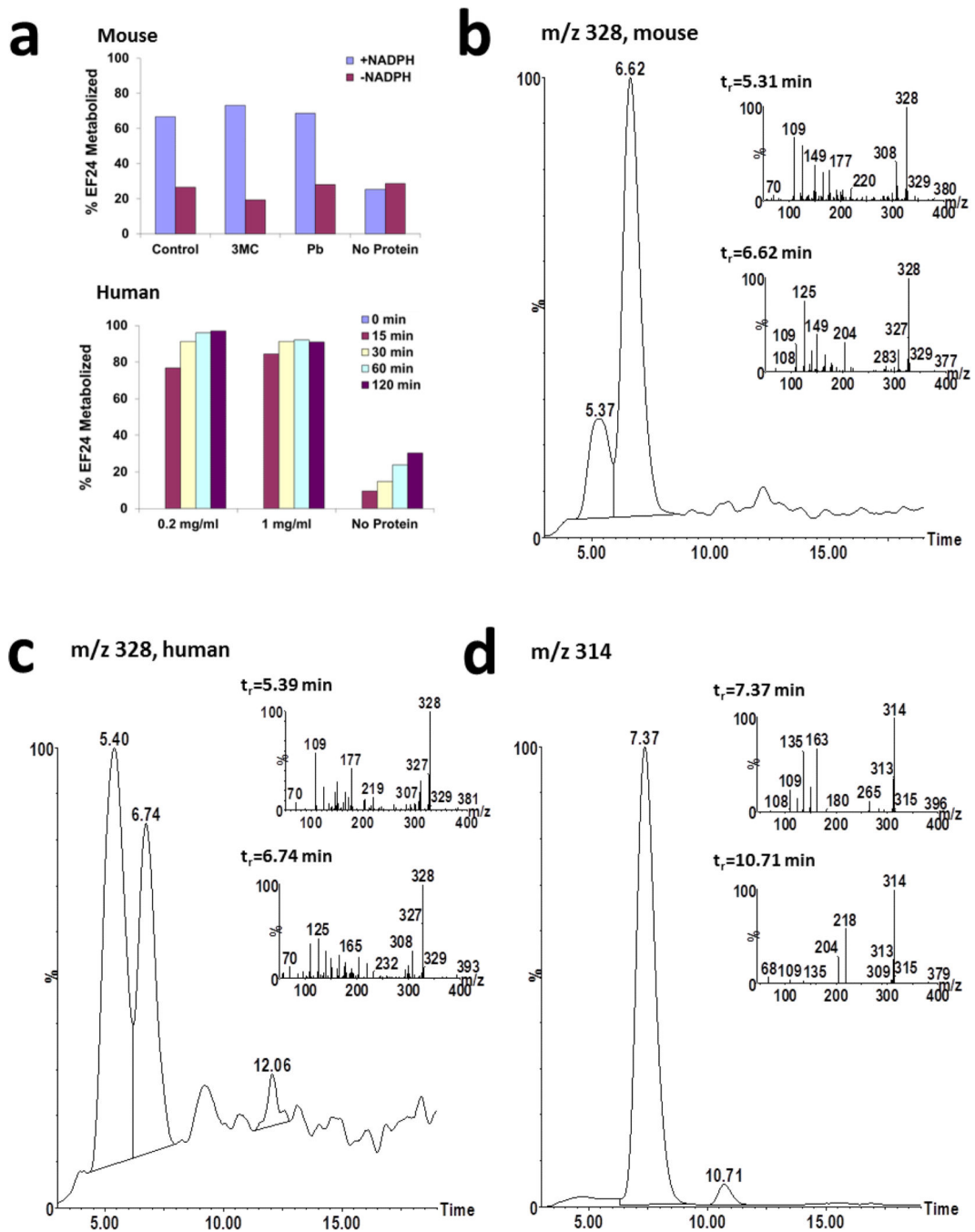


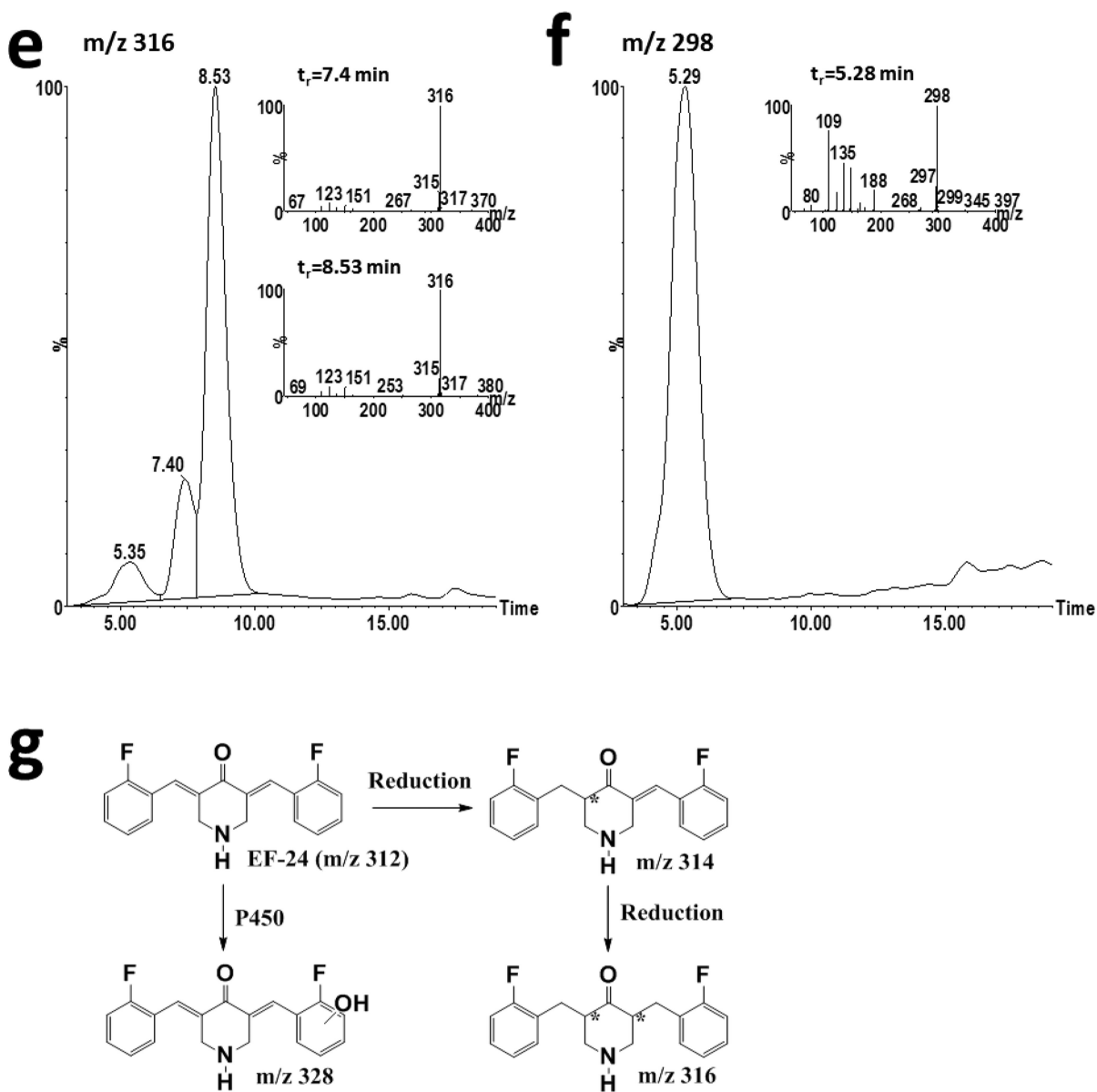
**Fig 2.**  
LC/MS/MS analysis of EF-24 and I-MAH-115. a) Fragmentation pattern produced by positive ESI of EF-24. b) Fragmentation pattern produced by positive ion ESI of I-MAH-115. c) Ion chromatogram of EF-24 in plasma extracts using the MRM transition 312.1>149.1. d) Ion chromatogram of I-MAH-115 in plasma extracts using the MRM transition 433.9>169





**Fig 3.** EF-24 plasma concentration-time profiles following intravenous (a), oral (b), or intraperitoneal (c) administration of 10 mg/kg EF-24 to male CD2F<sub>1</sub> mice



**Fig 4.**

In vitro metabolism of EF-24. a) EF-24 (10  $\mu$ M) was incubated with male CD2F1 mouse liver microsomes incubated for 15 minutes or human liver microsomes for 120 minutes in the presence or absence of NADPH. b) Ion chromatograms and daughter ion scans (inset) of putative hydroxylated metabolites with  $m/z$  328 formed during incubation of 100  $\mu$ M EF-24 with 3MC-pretreated male mouse liver microsomes. c) Ion chromatograms and daughter ion scans (inset) of putative hydroxylated metabolites with  $m/z$  328 formed during incubation of 100  $\mu$ M EF-24 with pooled human liver microsomes. d) Ion chromatograms and daughter ion scans (inset) of reduced EF-24 metabolites with  $m/z$  314 following incubation of EF-24 with pooled human liver microsomes. e) Ion chromatograms and daughter ion scans (inset) of reduced EF-24 metabolites with  $m/z$  316 following incubation of EF-24 with pooled human liver microsomes. f) Ion chromatogram and daughter ion scan (inset) of the unknown

metabolite with m/z 298. g) Scheme of EF-24 metabolism. The asterisk denotes chiral center(s) produced in the metabolites

Author Manuscript

Author Manuscript

Author Manuscript

Author Manuscript

**Table 1**

EF-24 Half-life in plasma (hours)

Concentration (nM)	31.25		1000	
	4°	37°	4°	37°
Human Plasma	84	79	100	58
Mouse Plasma	Stable	12	Stable	10
Rat Plasma	Stable	50	Stable	66
Dog Plasma	Stable	36	Stable	33

Author Manuscript

Author Manuscript

Author Manuscript

Author Manuscript

**Table 2**

Summary of pharmacokinetic estimates for EF-24 following administration of a 10 mg/kg dose.

	Intravenous	Oral	Intraperitoneal
T <sub>max</sub> , min	2.7	3	3
C <sub>max</sub> , nM	2494	882	833
t <sub>1/2α</sub> , min	0.4	3.3	8.9
t <sub>1/2β</sub> , min	5.4	--	--
t <sub>1/2z</sub> , min	73.6	177	219
AUC, nM•min	59730	35914	20734
Cl <sub>p</sub> , L/min/kg	0.482		
V <sub>ss</sub> , L/kg	4.85		
Bioavailability	-	60.1%	34.7%

Author Manuscript

Author Manuscript

Author Manuscript

Author Manuscript